Characterization of convection-related parameters by Raman lidar: Selected case studies from the convective and orographically-induced precipitation study

Paolo Di Girolamo, Donato Summa, and Dario Stelitano

Citation: AIP Conference Proceedings **1531**, 232 (2013); doi: 10.1063/1.4804749
View online: http://dx.doi.org/10.1063/1.4804749
View Table of Contents: http://scitation.aip.org/content/aip/proceeding/aipcp/1531?ver=pdfcov
Published by the AIP Publishing

Characterization of Convection-related Parameters by Raman Lidar: Selected Case Studies from the Convective and Orographically-induced Precipitation Study

Paolo Di Girolamo, Donato Summa and Dario Stelitano

Scuola di Ingegneria, Università della Basilicata, Viale dell'Ateneo Lucano n. 10, 85100 Potenza, Italy

Abstract. An approach to determine the convective available potential energy (CAPE) and the convective inhibition (CIN) based on the use of data from a Raman lidar system is illustrated in this work. The use of Raman lidar data allows to provide high temporal resolution measurements (5 min) of CAPE and CIN and follow their evolution over extended time periods covering the full cycle of convective activity. Lidar-based measurements of CAPE and CIN are obtained from Raman lidar measurements of the temperature and water vapor mixing ratio profiles and the surface measurements of temperature, pressure and dew point temperature provided by a surface weather station. The approach is applied to the data collected by the Raman lidar system BASIL in the frame of COPS. Attention was focused on 15 July and 25-26 July 2007. Lidar-based measurements are in good agreement with simultaneous measurements from radiosondes and with estimates from different mesoscale models.

Keywords: Lidar, Atmospheric stability, Temperature, Water vapor.
PACS: 92.60.e, 92.60.H, 42.68.Wt

INTRODUCTION

Several convection indices were designed in the past decades to describe the likelihood of convection or the type of convective systems that can be expected to occur [1,2]. Specifically, in order to indicate the potential for severe weather events, the convective available potential energy (CAPE) and the convective inhibition (CIN) can be determined.

Estimates of CAPE and CIN are traditionally determined from radiosonde data. The present paper proposes an approach to measure CAPE and CIN based on the use of lidar measurements of the temperature and water vapor mixing ratio profile and surface measurements of temperature, pressure and dew point temperature.

The convective inhibition index (CIN) is the energy that has to be provided to an air parcel in order to lift it vertically and dry-adiabatically from its initial position to its lifting condensation level (z_{LCL}) and then pseudo-adiabatically to its level of free convection (z_{LFC}). CIN represents the amount of negative buoyant energy available to inhibit upward vertical air acceleration. The largest is CIN the stronger must be the amount of forced lift to bring the parcel to its z_{LFC}. CIN can be defined as:

$$CIN = \int_{z_0}^{z_{LFC}} g \frac{T_p(z) - T(z)}{T(z)} \left[1 + 0.61 \cdot x_{H_2O}(z)\right] dz \left[J / kg_{ARIA}\right] \quad (1)$$

where the term $g\left[T_p(z) - T(z)/T(z)\right]$ represents the buoyant force per unit mass, with g being the gravitational acceleration (9,8076 m s-2), Tp(z) being the air parcel temperature at altitude z, T(z) being the environmental temperature at altitude z and $x_{H_2O}(z)$ is the water vapor mass mixing ratio (expressed in kg/kg); z_0 is the surface altitude. CIN can be calculated by vertically integrating the local buoyancy of the lifted air parcel from z_0 to z_{LFC} (red region in Fig. 1). It is to be specified out that the correction term in the square parenthesis allows to convert temperatures (both environmental and air parcel) into virtual temperatures.

When a layer of CIN is present, the layer must be eroded by surface heating or mechanical lifting, so that convective boundary layer parcels may reach their level of free convection (LFC). CIN and CAPE are both expressed in J/kg. Values of CIN below 50 J/kg indicate a weak cap that can be easily broken by surface heating, values between 50 and 200 indicate a moderate cap that can be broken by strong heating/synoptic scale forcing, while values in excess of 200 J/kg indicate a strong cap that prevents convection in the atmosphere and impedes thunderstorm development. nce z_{LFC} is reached by the lifting air parcel, CAPE can be released. CAPE is defined as:

Radiation Processes in the Atmosphere and Ocean (IRS2012)
AIP Conf. Proc. 1531, 232-235 (2013); doi: 10.1063/1.4804749

$$CAPE = \int_{zLFC}^{zEQL} g \frac{T_p(z) - T(z)}{T(z)} \left[1 + 0.61 \cdot x_{H_2O}(z)\right] dz \quad \left[J / kg_{ARIA}\right] \tag{2}$$

and can be calculated by vertically integrating the local buoyancy of the lifted air parcel from z_{LFC} to the equilibrium level (z_{EQL}) (green portion in Fig. 1).

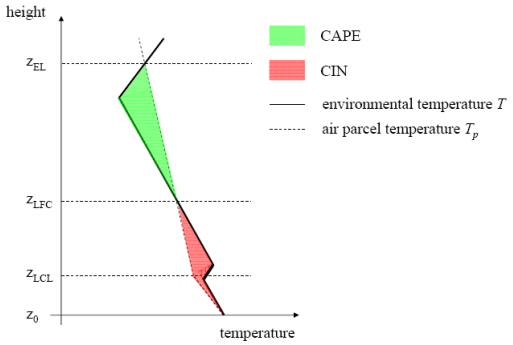

FIGURE 1. Schematic diagram representing the convection indices.

CAPE represents the positive buoyancy of the air parcel and is an indicator of atmospheric instability to a finite vertical displacement [3,4]. CAPE is widely used to quantify the maximum possible intensity of convection [5]: the larger is CAPE, the larger is the energy available for the formation of thunderstorm cells. CAPE exists within the conditionally unstable layer of the troposphere, where an ascending air parcel is warmer than the ambient air. Values of CAPE below 1000 J/kg indicate weak instability, values from 1000 to 2500 J/kg indicate moderate instability, while values larger than 2500 J/kg indicate strong instability.

To compute both CAPE and CIN a proper estimate of the lifting condensation level z_{LCL} is required. This is obtained from the surface values of atmospheric temperature, $T(z_0)$, and dew point temperature, $T_D(z_0)$, which, for the purpose of this work, are taken from a surface weather station. The dry-adiabatic lapse rate Γ_d has a constant value equal to –g/cp (0.009769 K/m), with cp being the specific heat at constant pressure (1004 J kg−1 K−1), while the pseudo-adiabatically lapse rate $\Gamma_s(z)$ varies with altitude and has a more complex formulation, which will be discussed at the conference, primarily dependent on the atmospheric temperature profile.

It is to be pointed out that deviations of temperature from virtual temperature have an very limited effect on the estimates of CIN and CAPE (< 1 %). Based on this consideration, in the present paper we are considering simplified expressions for CIN and CAPE which are including temperature instead of virtual temperature.

BASIL

The University of BASILicata Raman Lidar system (BASIL) was deployed in Achern (Black Forest, Germany, Lat: 48.64 °N, Long: 8.06 °E, Elev.: 140 m) in the frame of the Convective and Orographically-induced Precipitation Study (COPS) [6,7,8,9]. During COPS, BASIL operated between 25 May and 30 August 2007 and collected more than 500 hours of measurements, distributed over 58 measurement days and 34 intensive observation periods (IOPs).

The major feature of BASIL is its capability to perform high-resolution and accurate measurements of atmospheric temperature and water vapor, both in daytime and night-time, based on the application of the rotational and vibrational Raman lidar techniques in the UV [10,11,12,13,14,15]. Besides temperature and water vapor, BASIL provides measurements of the particle backscattering coefficient at 355, 532 and 1064 nm, of the particle extinction coefficient at 355 and 532 nm and of particle depolarization at 355 and 532 nm [12].

RESULTS AND DISCUSSION

We focused our attention on IOP 8b (15 July 2007), which was dedicated to the study of locally initiated convection or air-mass convection [8]. On 15 July 2007 deep convection developed on an area east of the Black Forest crest [16], although convective available potential energy was only moderate and convective inhibition was high in most of the COPS area. Data analysis revealed that synoptic forcing was absent and convection was triggered by different mechanisms [9].

The left panel of Fig. 2 illustrates the time evolution of the water vapor mixing ratio $x_{H_2O}(z)$ over a period of ~ 15 hours from 04:50 to 20:00 UT on 15 July 2007. The figure covers the daytime portion of the measurement record with noisy data above approximately 2-4 km. Fig. 2 is plotted as a succession of 5 min averaged consecutive profiles. The right panel of Fig. 2 illustrates the lidar measurements of the particle backscattering ratio at 1064 nm over the same ~ 15 hour period of Fig. 2. Vertical and temporal resolution of backscatter data are 15 m and 1 min, respectively.

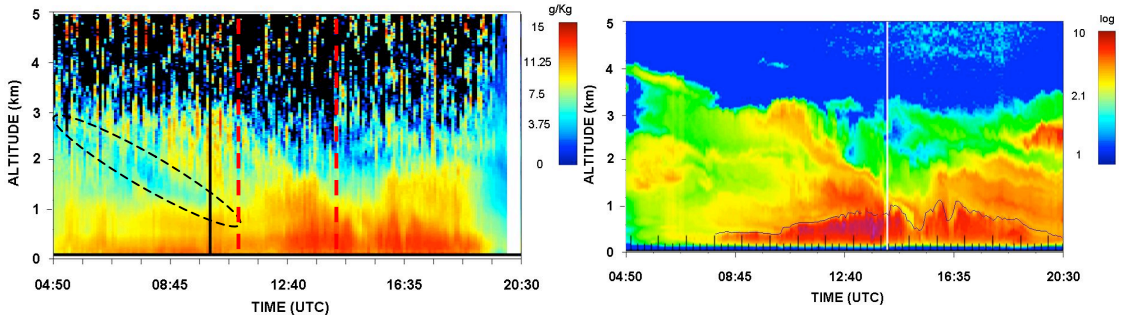

FIGURE 2. Left panel: Evolution of BASIL water vapor mixing ratio from 04:50 to 20:00 UT on 15 July 2007. The dashed ellipse highlights the presence of a dry layer acting as a lid and inhibiting convention. The dashed red line represents the times of the radiosoundings considered in this study. Right panel: Time evolution of the particle backscattering ratio at 1064 nm as measured by BASIL from 04:50 to 20:00 UT on 15 July 2007. Black line in the figure represents the PBL height as determined through the application of the algorithm illustrated by Summa et al. [17].

PBL height is illustrated in the figure as obtained through the application of the algorithm defined in [17]. The right panel of Fig. 3 illustrates the vertical profile of T and T_p, as obtained from data collected by the radiosonde launched in Achern at 10:59 UTC on 15 July 2007. The values of CAPE and CIN determined from the radiosonde data and obtained by considering the data up to the lid at approximately 6 km are 104 and -354 J/kg, respectively. The values of z_{LCL}, z_{LFC} and z_{EL} obtained from the radiosonde data are 1662 m, 3293 m and 5884, respectively. Values of CAPE and CIN obtained for this same radiosonde launch obtained by [9] are 90 and -327 J/kg, respectively, while those obtained by [18] are 86 and -219 J/kg, respectively.

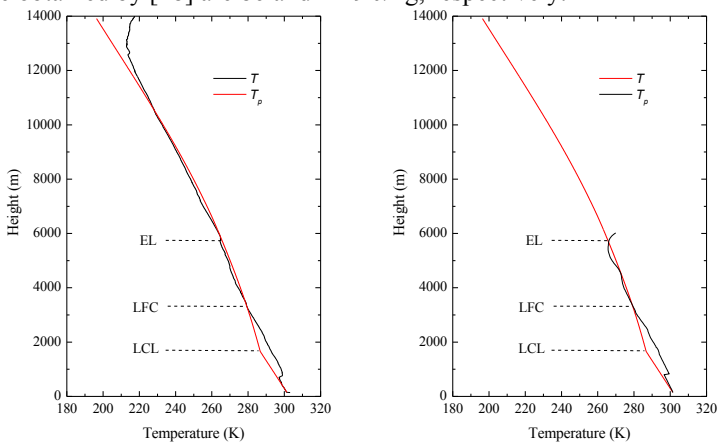

FIGURE 3: Left panel: Vertical profile of T and T_p, obtained from data collected by the radiosonde launched in Achern at 10:59 UTC on 15 July 2011. Right panel: Vertical profile of T and T_p, as obtained from the Raman lidar averaged over the time period 11:00-11:30 UTC on 15 July 2011.

The right panel of Fig. 3 illustrates the vertical profile of T, as measured by the Raman lidar, averaged over the time period 11:00-11:30 UTC on this same day (values above 6.1 km are not reported because affected by large random uncertainties). The figure also illustrates the vertical profile of T_p, as determined from Γ_d and $\Gamma_s(z)$, based on the Raman lidar measurement of T and the surface weather station measurements of $T(z_0)$, $p(z_0)$ and $T_D(z_0)$, for the same time period. Values of z_{LCL}, z_{LFC} and z_{EL} are 1637 m, 3200 m and 5900 m, respectively, in good agreement with those determined from the radiosonde data. The values of CAPE and CIN determined from the lidar measurements in the right panel of Fig. 3 are 92 and 360 J/kg, respectively, again in good agreement with those determined from the radiosonde data.

The left panel of Fig. 4 illustrates the evolution of CAPE and CIN over the time period 11:00-18:00 UTC on 15 July 2007 as determined from the lidar measurements. Values of CAPE are found to grow during the morning (up to approx. 1700 J/kg at 17:00 UTC) as a result of the increasing temperature and moisture in the PBL and the accumulation of potential convective energy. However, late in the morning and in the afternoon values of convective available potential energy were only moderate and convective inhibition was high (with slightly varying values around 200-300 J/kg). The high values of CIN inhibited deep convection on this day. As a result of this, shallow convective clouds only formed in the morning over the Vosges, but these diminished in the afternoon, while the rest of the COPS domain remained cloud-free.

Values of CIN and CAPE obtained from lidar and the radiosonde can also be compared with estimates from different mesoscale models. While the value of CAPE at 14:00 UTC from the lidar is 601 J/kg and from the radiosonde is 723 J/kg, corresponding value from WRF UK, Méso-NH, AROME and COSMO DLR are 711, 684, 664, 659 J/kg, respectively [18] (Table 1).

The above mentioned procedure was also tested for a night-time case study. The right panel of Fig. 4 illustrates the evolution of CAPE and CIN as over the time period 20:00-02:00 UTC on 25-26 July 2007. Values of CAPE and CIN keep stable and low as expected for convection free night-time conditions.

TABLE (1). Value of CAPE at 14:00 UTC from the lidar, the radiosonde and different mesoscale models.

Sonde	723 J/kg	Méso-NH	684 J/kg
Lidar	601 J/kg	AROME	664 J/kg
WRF UK	711 J/kg	COSMO-LR	659 J/kg

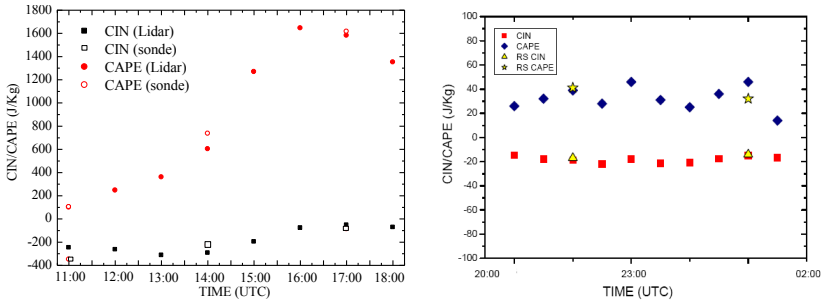

FIGURE 4: Left panel: Evolution of CAPE and CIN as over the time period 11:00-17:00 UTC on 15 July 2007 determined from the radiosonde and the lidar measurements. Right panel: Evolution of CAPE and CIN as over the time period 20:00-02:00 UTC on 25-26 July 2007 determined from the radiosonde and the lidar measurements.

REFERENCES

1. A. J. Haklander and A. Van Delden, *Atmos. Res*. **67-68**, 273–299 (2003).
2. M. Kunz, *Nat. Hazards Earth Syst. Sci*. **7**, 327–342 (2007).
3. A. Behrendt, M. Radlach, S. Pal and V. Wulfmeyer, 8th International Symposium on Tropospheric Profiling, 19 - 23 October 2009, Delft (2009).
4. U. Corsmeier et al., *Q. J. Roy. Meteorol. Soc*. **137**(S1), 137–155, doi:10.1002/qj.754 (2011).
5. K. A. Emanuel, *Atmospheric Convection*, New York: Oxford Univ. Press, 1994, 580 pp.
6. V. Wulfmeyer et al., *Bull. Am. Meteor. Soc*. **89**, 10, 1477-1486 (2008).
7. E. Richard et al., *La Météorologie* **64**, 32-42 (2009).
8. C. Kottmeier et al., *Meteorol. Z*. **17**, 6, 931-948 (2008).
9. N. Kalthoff et al., *Atmospheric Research* **93**, 4, 680-694 (2009).
10. P. Di Girolamo et al., *Geophysical Research Letters* **31**, L01106, doi:10.1029/2003GL018342 (2004).
11. P. Di Girolamo, A. Behrendt and V. Wulfmeyer, *Applied Optics* **45**, 11, 2474-2494, doi:10.1364/AO.45.002474 (2006).
12. P. Di Girolamo, D. Summa and R. Ferretti, *J. Atmos. Ocean. Tech*. **26**, 9, 1742–1762, doi:10.1175/2009JTECHA1253.1, (2009).
13. R. Bhawar et al., *Q. J. Roy. Meteorol. Soc*. **137**, 325–348, doi:10.1002/qj.697 (2011).
14. I. Fiorucci et al., *Journal of Geophysical Research* **113**, D14314, doi:10.1029/2008JD009831 (2008).
15. T. Maestri, P. Di Girolamo, D. Summa and R. Rizzi, *Atmospheric Research* **97**, 157–169 (2010).
16. E. Richard et al., *Q. J. Roy. Meteorol. Soc.* **137**, 101–117, doi: 10.1002/qj.710 (2011).
17. D. Summa, P. Di Girolamo and D. Stelitano, 26th International Laser Radar Conference, Porto Heli, Peloponnesus, Greece, June 25-29, (2012).
18. C. Barthlott et al., *Q. J. Roy. Meteorol. Soc.* **137**, 118–136, DOI: 10.1002/qj.707 (2011).